

# ornl



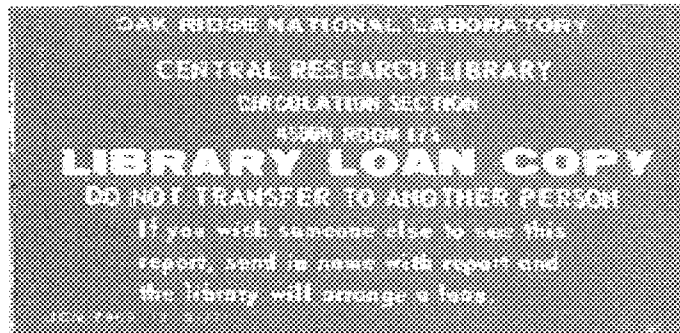
ORNL/TM-10207

OAK RIDGE  
NATIONAL  
LABORATORY

MARTIN MARIETTA

## Response of a Segmented Lead Glass Cerenkov Counter to (1-10 GeV) Incident Electrons, Gamma Rays and Hadrons

T. A. Gabriel  
B. L. Bishop



OPERATED BY  
MARTIN MARIETTA ENERGY SYSTEMS, INC.  
FOR THE UNITED STATES  
DEPARTMENT OF ENERGY

Printed in the United States of America. Available from  
National Technical Information Service  
U.S. Department of Commerce  
5285 Port Royal Road, Springfield, Virginia 22161  
NTIS price codes—Printed Copy: A03; Microfiche A01

This report was prepared as an account of work sponsored by an agency of the United States Government. Neither the United States Government nor any agency thereof, nor any of their employees, makes any warranty, express or implied, or assumes any legal liability or responsibility for the accuracy, completeness, or usefulness of any information, apparatus, product, or process disclosed, or represents that its use would not infringe privately owned rights. Reference herein to any specific commercial product, process, or service by trade name, trademark, manufacturer, or otherwise, does not necessarily constitute or imply its endorsement, recommendation, or favoring by the United States Government or any agency thereof. The views and opinions of authors expressed herein do not necessarily state or reflect those of the United States Government or any agency thereof.

ORNL/TM-10207

Engineering Physics and Mathematics Division

**Response of a Segmented Lead Glass Cerenkov Counter  
to (1-10 GeV) Incident Electrons, Gamma Rays and Hadrons**

T. A. Gabriel and B. L. Bishop\*

\*Computing & Telecommunications

Date Published: November 1986

Research sponsored by  
Office of High Energy and Nuclear Physics  
U. S. Department of Energy

Prepared by the  
Oak Ridge National Laboratory  
Oak Ridge, Tennessee 37831  
operated by  
Martin Marietta Energy Systems, Inc.  
for the  
U.S. DEPARTMENT OF ENERGY  
under Contract No. DE-AC05-84OR21400



3 4456 0147569 3



## TABLE OF CONTENTS

<b>Abstract</b> .....	<b>v</b>
<b>I. Introduction</b> .....	<b>1</b>
<b>II. Method of Calculation</b> .....	<b>1</b>
<b>III. Results</b> .....	<b>5</b>
<b>References</b> .....	<b>19</b>



### **Abstract**

The response of a segmented lead glass Cerenkov counter to (1-10 GeV) incident electrons, gamma rays and hadrons is studied using the CALOR computer system. The counter is divided into 30x30 modules each with a size of  $3.5 \times 3.5 \times 46 \text{ cm}^3$ . The calculated quantities include module cross talk, pulse height distributions with and without energy cuts.



**Response of a Segmented Lead Glass Cerenkov Counter  
to (1-10 GeV) Incident Electrons, Gamma Rays and Hadrons**

**T. A. Gabriel and B. L. Bishop**

## **I. Introduction**

Lead glass Cerenkov counters play a very important role in high-energy physics, especially in the detection of gamma rays and electrons. Their operation is based on the collection of the Cerenkov light emitted by the charged particles of the electromagnetic and hadronic showers. The number of photons emitted by the charged particles per unit path length is proportional to  $1 - [n(\nu)\beta]^{-2}$  where  $n(\nu)$  is the index of refraction for Cerenkov photons of frequency  $\nu$  and  $\beta$  is velocity of the charged particle. Typically, SF5 lead glass has an effective index of refraction in the frequency range of interest of 1.67 which yields a threshold energy value of 0.126 MeV for electrons and positrons. Electrons and positrons below this energy will not emit Cerenkov light. Charged muons, pions, and protons in a Cerenkov detector will have much higher threshold values due to their larger mass. Additional information on SF5 lead glass is included in Table 1.

Since lead glass counters are often used in mixed fields (leptons and hadrons) it becomes necessary to have a working knowledge of the response of the detector to both types of incident particles. Presented in this paper for a laterally segmented Cerenkov detector (30×30 modules 3.5×3.5×46 cm<sup>3</sup> each module) are data for 1-10 GeV incident electrons, photons, protons, and negatively charged pions. The data include pulse height distributions, cross-talk between adjacent modules, and the effect of threshold cuts on energy resolution and the previously mentioned calculated quantities. The method of calculation is presented in Section II and the results of the calculations are presented and discussed in Section III.

## **II. Method of Calculation**

The calculations performed with the CALOR computer system follow approximately the procedures used in previous calculations.<sup>1,2</sup> A flow diagram of the codes in CALOR is given in Fig. 1. The three-dimensional, multimedia, high-energy nucleon-meson transport code (HETC)<sup>3</sup> was used, with modifications, to obtain a detailed description of the nucleon-meson cascade produced in the devices considered in this paper. This Monte Carlo code takes into account the slowing down of charged particles via the continuous slowing-down approximation, the decay of charged pions and muons, inelastic nucleon-nucleus and charged-pion-nucleus (excluding hydrogen) collisions through the use of the intermediate-energy intranuclear-cascade-evaporation (MECC) model ( $E < 3$  GeV) and scaling model ( $E > 3$  GeV), and inelastic nucleon-hydrogen and charged-pion-hydrogen collisions via the isobar model ( $E < 3$  GeV) and phenomenological fits to experimental data ( $E > 3$  GeV). Also accounted for are elastic neutron-nucleus collisions ( $E < 100$  MeV), and elastic nucleon and charged-pion collisions with hydrogen.

**Table 1**  
**Composition of SF5 Pb/Glass**

<b>Material</b>	<b>Weight Fraction (g/cm<sup>3</sup>)</b>
SiO <sub>2</sub>	1.571
PbO	2.244
Na <sub>2</sub> O	0.082
K <sub>2</sub> O	0.163
	4.060

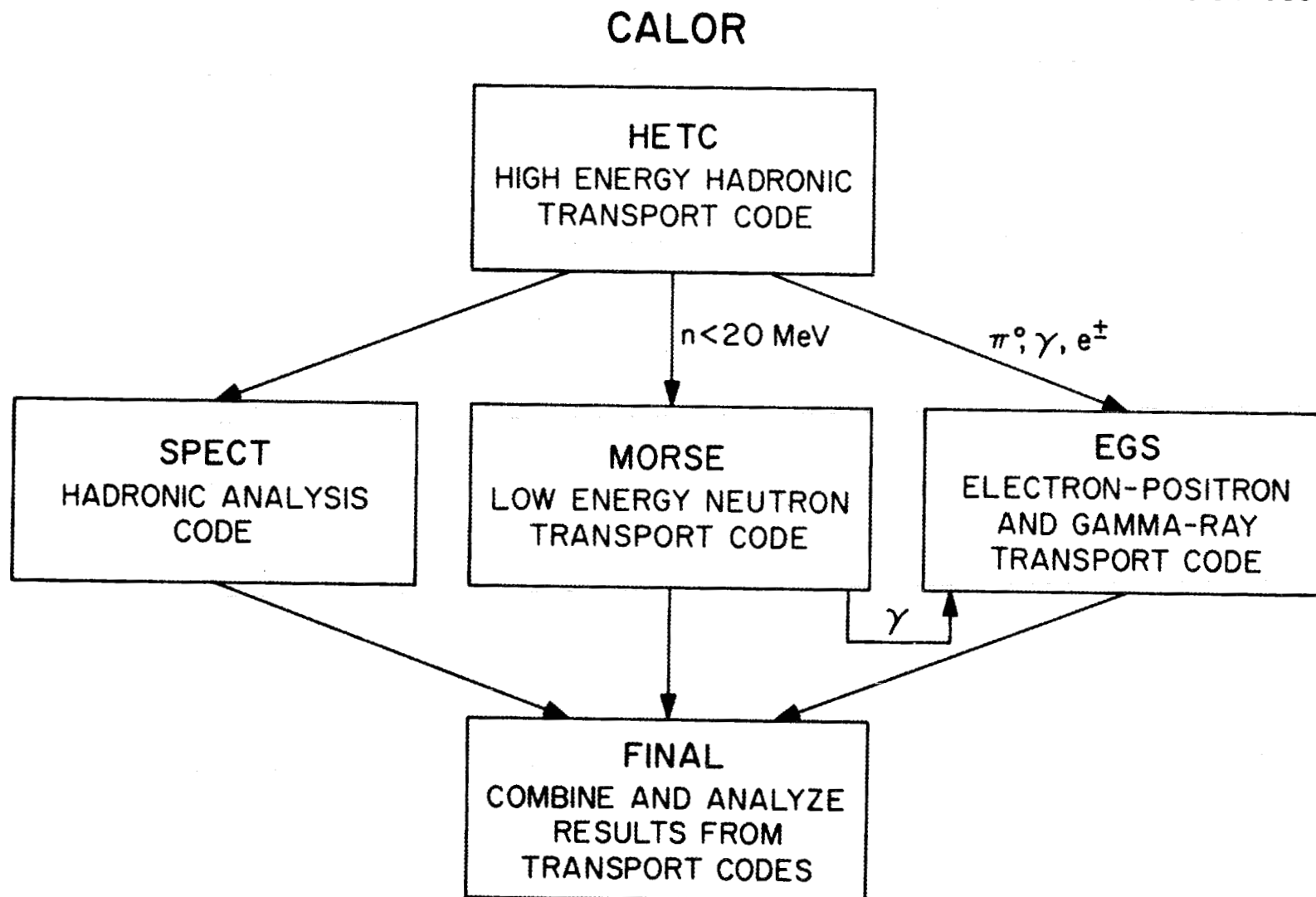


Fig. 1. Flow diagram of the CALOR computer system.

The intranuclear-cascade-evaporation model as implemented by Bertini is the heart of the HETC code.<sup>4</sup> This model has been used for a variety of calculations and has been shown to agree quite well with many experimental results. Even when agreement is not very good, the results produced by this model can lead the user to make correct decisions. The underlying assumption of this model is that particle-nuclear interactions can be treated as a series of two-body collisions within the nucleus and that the location of the collision and resulting particles from the collision are governed by experimental and/or theoretical particle-particle total and differential cross-section data. The types of particle collisions included in the calculations are elastic, inelastic and charge exchange. This model incorporates the diffuseness of the nuclear edge, the Fermi motion of the bound nucleons, the exclusion principle, and a local potential for nucleons and pions. The density of the neutrons and protons within the nucleus (which is used with the total cross section to determine interaction locations) are determined from the experimental data of Hofstadter.<sup>4</sup> Nuclear potentials are determined from these density profiles by using a zero-temperature Fermi distribution. The total well depth is then defined as the Fermi energy plus 7 MeV. Following the cascade part of the interaction, there is excitation energy left in the nucleus. This energy is treated by using an evaporation model which allows for the emission of protons, neutrons, d, <sup>3</sup>He,  $\alpha$ , and T. Fission induced by high-energy particles is accounted for during this phase of the calculation by allowing it to compete with evaporation. Whether or not a detailed fission model is included has very little effect on the total number of secondary neutrons produced.

The source distribution for the electromagnetic cascade calculation is provided by HETC; it consists of photons from neutral pion decay, electrons and positrons from muon decay (although this is usually not of interest in calorimeter calculations because of the long muon lifetime), deexcitation gamma rays from inelastic nuclear collisions, and fission gamma rays. Since the discrete decay energies of the deexcitation gammas are not provided by HETC and only the total energy is known, individual gamma energies are obtained by uniformly sampling from the available energy until it is completely depleted. The transport of the electrons, positrons, and gammas from the above sources is carried out using the EGS system.<sup>5</sup>

Neutrons which are produced with energies below 20 MeV are transported using the MORSE<sup>6,7</sup> Monte Carlo transport code. The neutron cross sections used by MORSE were obtained from ENDFB/IV. Gamma rays (including those from capture, fission, etc.) produced during this phase of the calculations are stored for transport by the EGS code. The MORSE code was developed for reactor application and can treat fissioning systems in detail. This ability is very important since a majority of the fission compensation results from neutrons with energies less than 20 MeV. Time dependence is included in MORSE, but since neither HETC nor EGS has a timing scheme incorporated, it has been assumed that no time passes for this phase of the particle cascade. Therefore, all neutrons below 20 MeV are produced at  $t = 0$ . General time cuts used in the MORSE code are 50 nsec for scintillator and Cerenkov counters and 100 nsec for liquid argon counters.

The Cerenkov light pulse is obtained for hadrons from the following equation

$$I = \int_{E_1}^{E_2} C \left( 1 - \frac{1}{\beta^2 n^2} \right) \frac{dE}{dE/dx}$$

and for electrons and positrons  $I = C(1 - 1/\beta^2 n^2)\Delta x$ . The overall normalized  $C$  is determined relative to 1 GeV incident gamma rays. The peak of this pulse height is defined as 1 GeV. All particles are normally incident at the center of the center module. Since light collection statistics dominates the energy resolution all pulse height distributions have incorporated a smearing function so that the resolution of a 1 GeV incident gamma ray is 12% ( $\sigma/E = 12\%/\sqrt{E}$ ) with no energy threshold cut.

### III. Results

In many EGS calculations the cutoff energy of the electron/positron is sometimes set very high, on the order of several MeV, so as to speed up the calculation. However, caution should be applied when high cutoffs are used. The results in Fig. 2 show the relative change in the average Cerenkov signal for 1 GeV incident gamma rays when the cutoff energy is progressively increased. Approximately 20% of the Cerenkov signal results from electrons with energies between 1.0 MeV and the Cerenkov threshold of 0.126 MeV.

The average Cerenkov pulses in the lead glass arrays are given in Tables 2-8 for 1-, 5-, and 10-GeV incident gamma rays and protons and for 1-GeV incident negative pions. The numbers in the B tables represent the average signals when 50 MeV energy cuts are imposed on each lead glass module; i.e., the signal in each lead glass module must be greater than 50 MeV before it is used in calculating the average. The other numbers have no energy cuts.

Substantial cross-talk between adjacent modules is evident in all of the tables. The data for the incident gamma rays will sum approximately to the incident gamma ray energies. The higher gamma ray energy sum will be slightly less due to energy leakage. The average signals for the incident hadrons will sum to values substantially lower due to leakage energy, to energy lost in neutron production, and to the production of charged particles below the Cerenkov production energy.

The effect of energy cuts on the average Cerenkov signal and energy resolution is present in Table 9. Percentagewise the energy cuts have the largest effect on the 1-GeV electron and gamma ray data both for energy deposition and resolution.

The pulse height distributions integrated over all modules for 1-, 5-, and 10-GeV incident electrons, negatively charged pions, and protons are presented in Figs. 3-5. The large pulse heights in the hadron cases at approximately 300 MeV are due to noninteracting primary particles punching through. The 1- and 5-GeV proton pulse height distributions with 50-MeV energy cuts on each module are also indicated as points in Figs. 3 and 4.

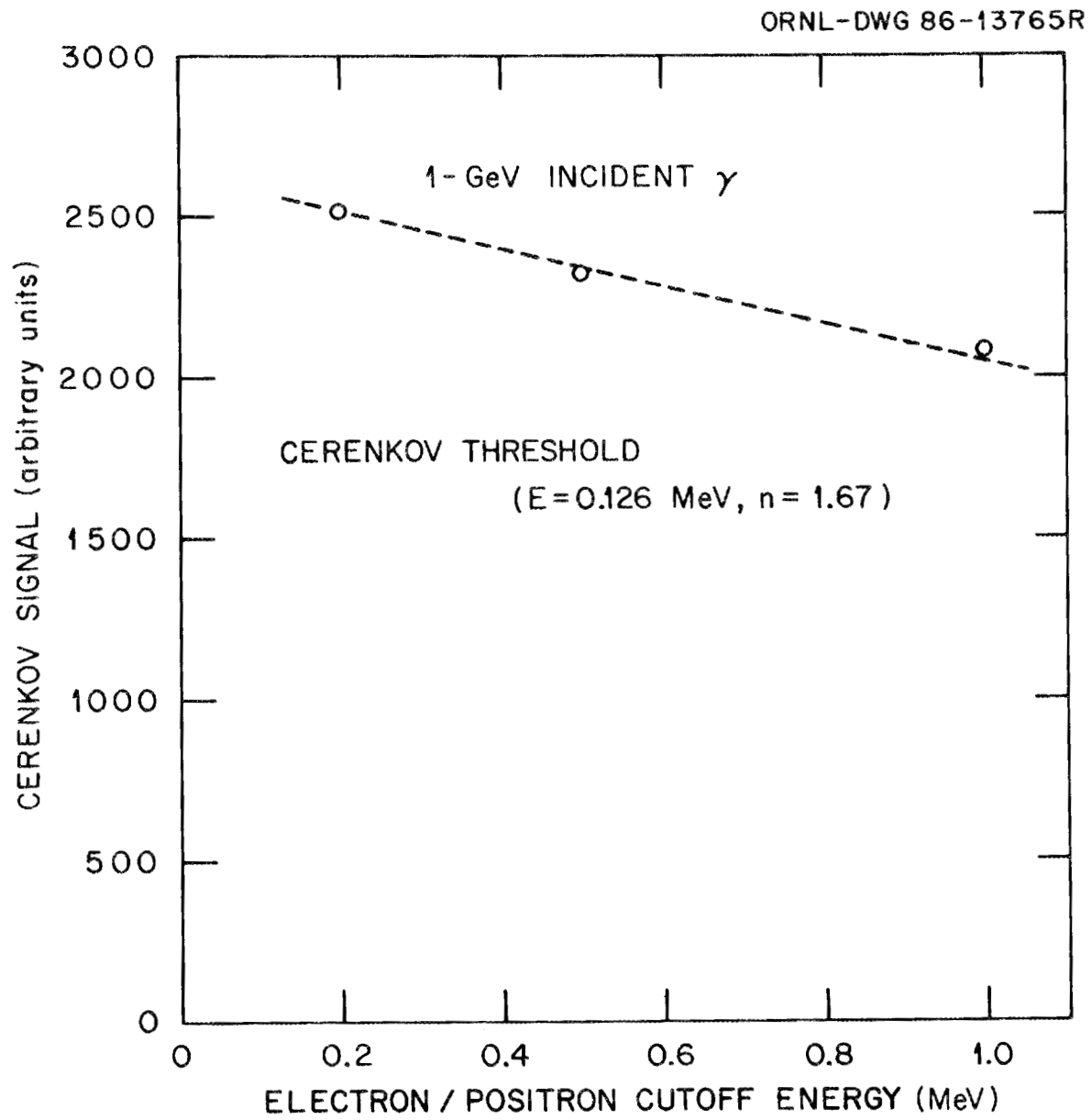


Fig. 2. Effect of energy on Cerenkov pulse.

<b>Table 2.A</b>						
<b>Average Cerenkov pulse (MeV) in Pb-glass array</b>						
<b>1-GeV gamma rays incident on center Pb-glass block</b>						
0.1	0.4	0.6	0.8	0.6	0.3	0.3
0.2	0.8	2.1	3.4	2.0	1.0	0.4
0.6	2.0	9.6	29.1	9.9	1.8	0.6
0.7	3.2	26.7	788.	29.9	2.8	0.7
0.5	2.1	8.9	28.9	10.2	2.1	0.6
0.3	0.8	1.9	3.2	1.9	0.8	0.3
0.1	0.4	0.5	0.9	0.6	0.2	0.2

<b>Table 2.B</b>				
<b>Average Cerenkov pulse (MeV) in Pb-glass array</b>				
<b>1-GeV gamma rays incident on center Pb-glass block</b>				
<b>with a 50 MeV energy cut on each Pb-glass module</b>				
0.0	1.1	13.4	0.8	0.0
0.2	11.7	787.	13.0	0.1
0.1	1.0	11.8	1.6	0.0

Table 3								
Average Cerenkov pulse (MeV) in Pb-glass array								
1-GeV $\pi^-$ incident on center Pb-glass block								
0.5	0.2	0.4	0.4	0.5	0.4	0.3	0.3	0.1
0.2	0.7	0.8	0.8	1.1	1.1	0.6	0.4	0.1
0.4	1.0	1.4	2.0	2.7	2.5	1.0	0.5	0.5
1.1	1.4	3.0	5.8	8.6	5.2	2.0	1.2	0.5
0.6	1.2	2.4	8.7	195.	11.0	3.5	1.7	1.4
0.6	1.3	2.3	4.7	9.1	6.6	2.3	1.4	0.9
0.4	0.8	1.3	2.1	3.6	2.2	1.4	0.5	0.4
0.2	0.9	0.8	1.3	1.4	0.9	0.9	0.7	0.2
0.4	0.2	0.4	0.5	0.6	0.3	0.4	0.4	0.3

<b>Table 4.A</b>						
<b>Average Cerenkov pulse (MeV) in Pb-glass array</b>						
<b>1-GeV protons incident on center Pb-glass block</b>						
0.1	0.2	0.4	0.5	0.5	0.2	0.1
0.2	0.3	1.2	1.2	1.1	0.3	0.2
0.3	0.7	2.2	4.7	2.6	0.9	0.4
0.5	1.1	4.9	141.	3.6	1.1	0.7
0.3	1.0	2.9	4.2	2.6	0.9	0.4
0.3	0.7	1.0	1.0	1.0	0.5	0.4
0.1	0.2	0.3	0.3	0.2	0.2	0.1

<b>Table 4.B</b>						
<b>Average Cerenkov pulse (MeV) in Pb-glass array</b>						
<b>1-GeV protons incident on center Pb-glass block</b>						
<b>with a 50 MeV energy cut on each Pb-glass module</b>						
0.0	0.0	0.4	0.4	0.4	0.0	0.0
0.0	0.1	0.9	2.2	0.9	0.1	0.0
0.1	0.2	2.6	137.	1.6	0.2	0.3
0.0	0.2	1.4	1.8	1.2	0.2	0.0
0.0	0.0	0.3	0.2	0.2	0.0	0.2

<b>Table 5.A</b>										
<b>Average Cerenkov pulse (MeV) in Pb-glass array</b>										
<b>5-GeV gamma rays incident on center Pb-glass block</b>										
0.1	0.1	0.2	0.4	0.6	0.5	0.5	0.3	0.1	0.1	0.1
0.2	0.3	0.5	0.8	1.2	1.2	0.8	0.7	0.4	0.3	0.1
0.1	0.4	1.0	2.0	3.4	3.9	2.7	2.2	1.1	0.5	0.2
0.3	0.7	1.7	4.6	8.7	13.0	9.9	4.3	1.8	0.7	0.4
0.3	1.3	2.6	8.9	45.3	136.	47.6	9.6	3.0	0.9	0.2
0.5	0.9	3.1	13.6	127.	3923.	148.	15.8	4.2	1.3	0.6
0.2	1.1	3.0	9.3	44.9	148.	48.9	11.3	2.9	1.3	0.4
0.4	0.6	1.9	3.8	9.0	14.8	10.6	4.7	2.0	0.8	0.3
0.2	0.4	0.7	1.7	3.1	3.1	3.2	2.4	0.7	0.4	0.2
0.0	0.1	0.4	0.6	1.3	1.2	1.1	0.8	0.6	0.1	0.2
0.1	0.1	0.2	0.4	0.5	0.6	0.5	0.3	0.1	0.1	0.0

<b>Table 5.B</b>				
<b>Average Cerenkov pulse (MeV) in Pb-glass array</b>				
<b>5-GeV gamma rays incident on center Pb-glass block</b>				
<b>with a 50 MeV energy cut on each Pb-glass module</b>				
0.0	0.1	0.6	0.0	0.0
0.3	26.2	135.	29.1	0.1
0.7	126.	3923.	147.	1.0
0.0	25.6	147.	30.5	1.0
0.0	0.4	1.1	0.3	0.0

<b>Table 6.A</b>										
<b>Average Cerenkov pulse (MeV) in Pb-glass array</b>										
<b>5-GeV protons incident on center Pb-glass block</b>										
0.1	0.2	0.4	0.4	0.5	0.5	0.7	0.4	0.3	0.2	0.1
0.3	0.3	0.5	0.8	1.1	1.4	1.4	1.0	0.3	0.4	0.2
0.3	0.6	1.3	1.5	2.5	3.7	3.4	2.1	1.1	0.6	0.3
0.4	0.9	1.9	4.5	6.2	10.5	7.1	4.1	1.8	1.0	0.5
0.5	1.1	3.0	6.6	20.8	38.0	21.4	6.8	2.9	1.6	0.7
0.4	1.4	3.3	9.6	43.6	325.	40.2	8.2	2.7	1.3	0.5
0.6	1.0	2.9	9.3	25.9	40.2	21.2	7.2	3.2	1.0	0.5
0.3	1.0	2.3	4.9	9.4	9.0	6.9	3.3	2.0	0.8	0.6
0.3	1.0	1.5	2.4	3.7	3.1	2.8	1.4	1.0	0.8	0.3
0.3	0.6	0.9	1.3	1.6	1.1	1.4	0.7	0.4	0.4	0.2
0.2	0.4	0.5	0.5	0.8	0.6	0.5	0.3	0.3	0.2	0.2

Table 6.B										
Average Cerenkov pulse (MeV) in Pb-glass array										
5-GeV protons incident on center Pb-glass block										
with a 50 MeV energy cut on each Pb-glass module										
0.0	0.0	0.1	0.0	0.0	0.1	0.1	0.0	0.0	0.0	0.0
0.1	0.0	0.1	0.0	0.2	0.5	0.4	0.2	0.0	0.1	0.0
0.1	0.1	0.3	0.3	0.8	1.9	1.7	0.7	0.3	0.0	0.0
0.0	0.1	0.7	2.4	3.4	7.1	4.2	2.2	0.6	0.4	0.1
0.0	0.2	1.0	3.3	15.8	32.5	17.2	3.8	1.2	10.5	0.2
0.1	0.3	1.4	6.3	37.5	325.	34.8	4.7	0.8	0.4	0.0
0.1	0.0	1.0	6.3	21.3	35.1	16.5	4.1	1.7	0.3	0.1
0.0	0.2	0.7	2.4	6.3	5.8	4.1	1.3	0.8	0.2	0.1
0.0	0.4	0.5	0.9	1.9	1.1	1.2	0.5	0.2	0.2	0.0
0.0	0.1	0.2	0.5	0.5	0.3	0.4	0.1	0.0	0.1	0.0
0.0	0.0	0.1	0.0	0.1	0.1	0.0	0.0	0.1	0.0	0.0

Table 7												
Average Cerenkov pulse (MeV) in Pb-glass array												
10-GeV gamma rays incident on center Pb-glass block												
0.0	0.2	0.2	0.2	0.3	0.4	0.5	0.3	0.3	0.2	0.0	0.0	0.0
0.0	0.1	0.3	0.3	0.6	0.9	0.6	0.8	0.5	0.4	0.2	0.1	0.2
0.2	0.2	0.5	0.9	1.6	2.0	2.5	1.9	1.7	1.0	0.6	0.3	0.1
0.3	0.4	1.0	1.9	3.1	5.8	7.2	6.0	3.9	2.0	1.2	0.4	0.1
0.3	0.7	1.5	3.9	8.4	18.6	27.7	18.6	7.7	3.3	1.9	0.5	0.2
0.3	0.9	2.1	6.7	17.6	87.0	262.	88.5	20.4	6.0	2.6	0.8	0.3
0.4	1.0	2.4	8.0	29.1	269.	7806.	288.	27.2	7.3	2.8	1.1	0.3
0.5	1.2	2.2	5.9	19.3	87.5	282.	93.2	20.7	6.4	2.1	0.8	0.4
0.4	0.7	1.7	3.7	7.7	17.9	27.1	20.3	8.1	3.5	1.3	0.9	0.3
0.2	0.5	0.9	1.7	3.3	5.7	6.4	5.7	4.2	1.8	0.9	0.5	0.1
0.2	0.3	0.6	0.9	1.5	2.2	2.6	2.3	1.6	0.9	0.6	0.4	0.1
0.1	0.2	0.1	0.6	0.9	0.9	0.9	0.8	0.9	0.3	0.2	0.1	0.1
0.0	0.1	0.1	0.2	0.3	0.2	0.5	0.4	0.5	0.3	0.1	0.0	0.0

Table 8										
Average Cerenkov pulse (MeV) in Pb-glass array										
10-GeV protons incident on center Pb-glass block										
0.2	0.3	0.4	0.5	0.4	0.7	0.6	0.6	0.3	0.3	0.1
0.3	0.5	1.0	1.1	1.3	1.8	1.8	0.9	0.8	0.4	0.2
0.3	0.8	1.8	2.9	4.2	4.8	4.5	2.8	1.6	0.7	0.3
0.6	1.1	3.0	6.0	12.6	14.4	12.1	6.9	2.8	1.6	1.0
0.6	1.6	4.6	13.7	44.0	77.5	40.3	14.1	4.5	1.6	1.0
0.6	1.5	4.6	16.5	84.8	551.	84.1	15.4	4.6	1.6	1.0
0.9	1.6	3.7	13.7	47.0	82.8	47.7	13.8	4.3	1.5	0.7
0.8	1.3	2.7	6.7	12.4	19.6	13.8	8.4	3.2	1.2	0.4
0.4	0.7	1.6	2.7	5.3	5.8	4.4	3.0	1.7	0.9	0.4
0.1	0.2	0.6	1.3	2.6	2.3	1.7	1.1	0.8	0.5	0.2
0.1	0.4	0.5	0.7	1.1	0.9	1.0	0.4	0.3	0.3	0.2

Table 9

Effect of energy cuts on average Cerenkov signal and energy resolution

Energy Cut (MeV)	Average Signal (MeV)					
	1-GeV		5-GeV		10-GeV	
	e <sup>-</sup>	Gamma	e <sup>-</sup>	Gamma	e <sup>-</sup>	Gamma
0.	999.	999.	4952.	4931.	9851.	9777.
2.	989.	989.	4932.	4910.	9825.	9751.
4.	977.	977.	4904.	4883.	9789.	9715.
10.	947.	947.	4834.	4812.	9696.	9621.
20.	910.	910.	4750.	4731.	9575.	9498.
50.	843.	842.	4608.	4595.	9360.	9282.
Energy Resolution ( $\Delta E/E\%$ )						
0.	11.8	12.0	5.3	5.4	4.2	4.1
2.	11.9	12.4	5.3	5.4	4.2	4.1
4.	12.2	12.6	5.4	5.4	4.2	4.1
10.	12.7	13.4	5.5	5.5	4.2	4.1
20.	13.9	14.6	5.6	5.6	4.3	4.1
50.	17.1	17.7	6.0	5.9	4.7	4.2

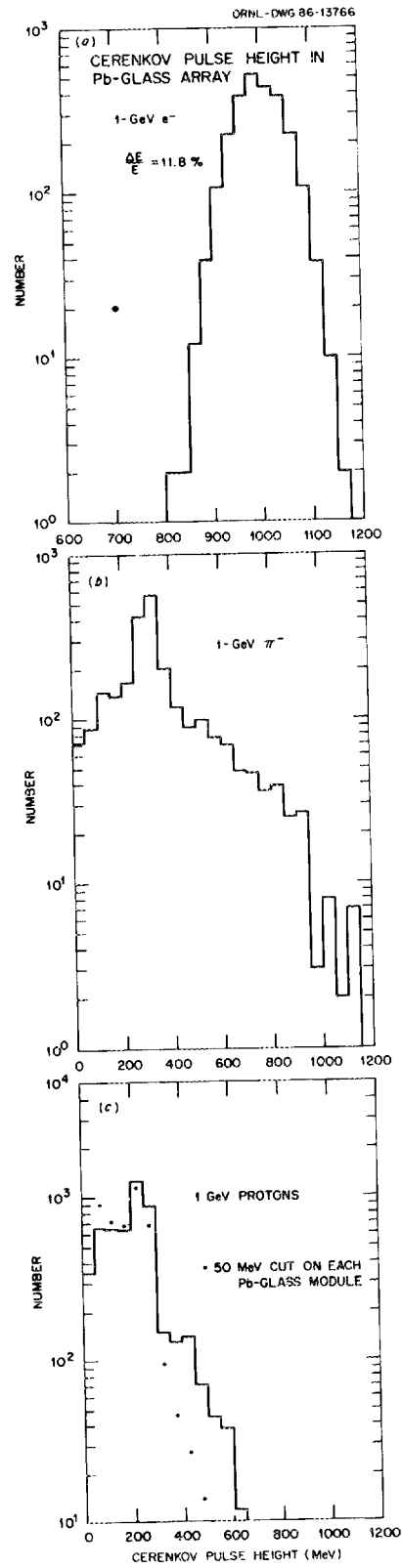


Fig. 3. Cerenkov pulse height distributions for 1-GeV incident electrons, negatively charged pions, and protons.

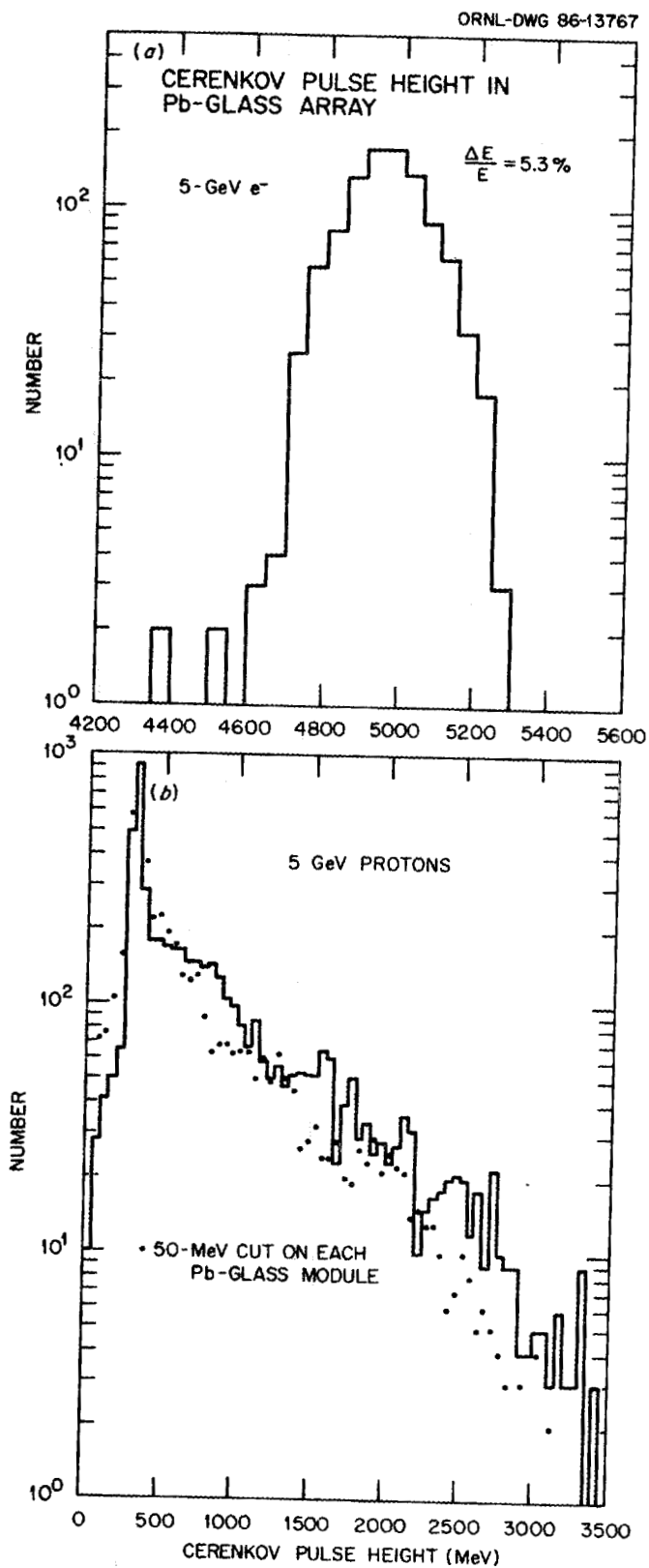


Fig. 4. Cerenkov pulse height distributions for 5-GeV incident electrons and protons.

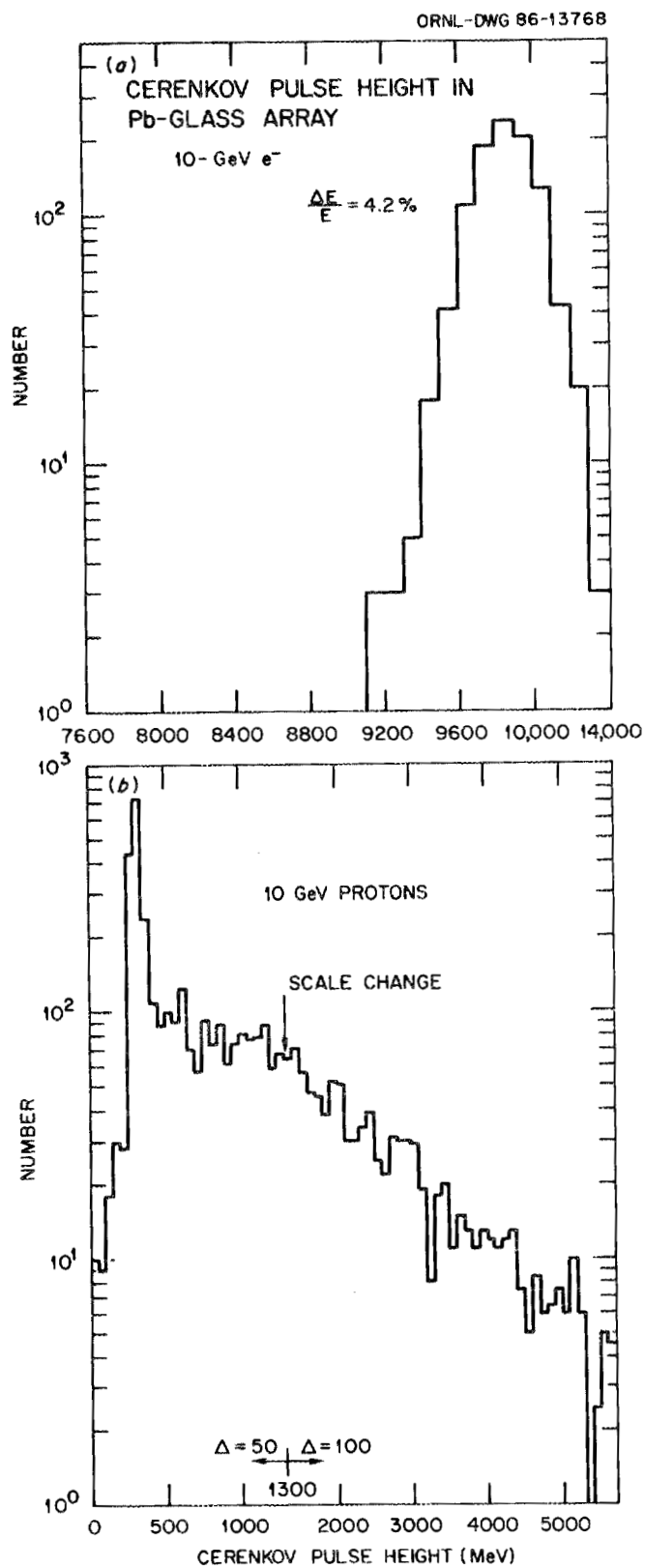


Fig. 5. Cerenkov pulse height distributions for 10-GeV incident electrons and protons.

**References**

1. T. A. Gabriel and W. Schmidt, *Nucl. Instrum. Methods* **134**, 271 (1976).
2. T. A. Gabriel, *Nucl. Instrum. Methods* **150**, 146 (1978).
3. K. C. Chandler and T. W. Armstrong, "Operating Instructions for the High-Energy Transport Code HETC," ORNL-4744, Oak Ridge National Laboratory (1972).
4. H. W. Bertini, *Phys. Rev.* **188**, 1711 (1969).
5. R. L. Ford and W. R. Nelson, "The EGS Code System Computer Programs for the Monte Carlo Simulation of Electromagnetic Cascade Showers (Version 3)," SLAC-0210 (1978).
6. M. B. Emmett, "The MORSE Monte Carlo Radiation Transport Code System," ORNL-4972, Oak Ridge National Laboratory (1975).
7. N. M. Greene et al., "AMPX: A Modular Code System for Generating Coupled Multigroup Neutron-Gamma Libraries from ENDF/B," ORNL/TM-3706, Oak Ridge National Laboratory (1973).



*INTERNAL DISTRIBUTION*

- |        |                      |        |   |
|--------|----------------------|--------|---|
| 1.     | F. S. Alsmiller      | 20.    | P. W. Dickson, Jr. (Consultant)                           |
| 2.     | R. G. Alsmiller, Jr. | 21.    | G. H. Golub (Consultant)                                  |
| 3-8.   | B. L. Bishop         | 22.    | R. Haralick (Consultant)                                  |
| 9-12.  | T. A. Gabriel        | 23.    | D. Steiner (Consultant)                                   |
| 13-14. | R. A. Lillie         | 24-25. | Central Research Library                                  |
| 15.    | F. C. Maienschein    | 26.    | ORNL Y-12 Technical Library<br>Document Reference Section |
| 16.    | R. W. Peelle         | 27-28. | Laboratory Records  |
| 17.    | RSIC                 | 29.    | ORNL Patent Office  |
| 18.    | R. T. Santoro        | 30.    | Laboratory Records - RC                                   |
| 19.    | A. Zucker            |        |   |

*EXTERNAL DISTRIBUTION*

31. Office of Assistant Manager for Energy Research & Development, DOE-ORO, Oak Ridge, TN 37830
32. Argonne National Laboratory, Library Services Department, 302-CE125, 9700 S. Cass Avenue, Argonne, IL 60439
33. T. W. Armstrong, Science Applications, Inc., PO Box 2807, La Jolla, CA 92038
34. Miguel Awschalom, National Accelerator Laboratory, PO Box 500, Batavia, IL 60510
35. V. S. Barashenkov, Laboratory of Theoretical Physics, Joint Institute for Nuclear Research, Head Post Office, PO Box 79, Moscow, USSR
36. Brookhaven National Laboratory, Attention: Research Library, Upton, NY 11973
37. L. S. Cardman, Nucl. Phys. Lab., 23 Stadium Dr., Champaign, IL 61820
38. Stanley B. Curtis, Lawrence Radiation Laboratory, Bldg. 29, Room 213, Berkeley, CA 94720

39. Herbert Destaebler, Stanford Linear Accelerator Center, Stanford University, Stanford, CA 94305
40. R. D. Edge, Physics Department, University of South Carolina, Columbia, SC 29208
41. Dr. R. Eisenstein, Department of Physics, University of Illinois, Urbana, IL 61801
42. H. T. Freudenreich, University of Maryland, College Park, MD 20742
43. E. Freytag, Deutsches Elektronen-Synchrotron, DESY, 2 Hamburg Dr., Flottbek, Notkesteig 1, W. Germany
44. Dr. G. T. Gillies, Department of Physics, University of Virginia, Charlottesville, VA 22901
45. Dr. Gary E. Gladding, University of Illinois, Department of Physics, Urbana, IL 61801
46. K. Goebel, Health Physics Group, CERN, 1211 Geneva 23, Switzerland
47. J. A. Goodman, University of Maryland, College Park, MD 20742
48. Dr. Herman Grunder, CEBAF, 12070 Jefferson Ave., Newport News, VA 23606
49. Frenc Hajnal, Health and Safety Laboratory, U.S. Department of Energy, 376 Hudston St., NY, NY 10014
50. M. Hofert, CERN, 1211 Geneva 23, Switzerland
51. Dr. Inga Karliner, Physics Dept., University of Illinois, Urbana, IL 61801
52. Prof. D. Lal, Tata Institute of Fundamental Research, National Centre of the Government of India for Nuclear Science & Mathematics, Homi Bhabha Rd., Bombay 5, India
53. Lawrence Livermore Laboratory, Technical Information Department, PO box 808, Livermore, CA 94550
54. V. Lebedev, Institute of High Energy Physics, Serpukhov, Moscow Region, USSR

55. Library for Nuclear Science, Massachusetts Institute of Technology at Middleton, Middleton, MA 01949
56. Dr. J. Marks, Accelerator Fusion Research Division, Lawrence Berkeley Laboratory, Bldg. 50, Room 149, 1 Cyclotron Rd., Berkeley, CA 94720
57. Dr. V. S. Narasimham, Tata Institute of Fundamental Research, Bombay 400 005, India
58. W. R. Nelson, Stanford Linear Accelerator Center, Stanford University, PO Box 4349, Stanford, CA 94305
59. Keran O'Brien, Health and Safety Laboratory, U.S. Department of Energy, 376 Hudson St., NY, NY 10014
60. J. Ranft, Karl-Marx University, Physics Section, Linnestrasse 5, 701 Leipzig, W. Germany
61. Dr. Lincoln Reed, Division of High Energy and Nuclear Physics, Department of Energy, Washington, DC 20545
62. The Secretary, Radiation Group, Lab II, CERN, 1211 Geneva 23, Switzerland
63. B. S. P. Shen, Department of Astronomy, University of Pennsylvania, Philadelphia, PA 19104
64. Dr. M. Shupe, Department of Physics, University of Minnesota, Minneapolis, MN 55455
65. Stanford Linear Accelerator Center, Attention: Library, PO Box 4349, Stanford, CA 94305
66. Dr. Alan Stevens, Accelerator Dept. Bldg. 911, Brookhaven National Laboratory, Upton, NY 11973
67. G. R. Stevenson, Radiation Protection Group, Lab II, CERN, 1211 Geneva 23, Switzerland
68. R. Tesch, DESY, Hamburg, Notkesteig 1, W. Germany
69. Ralph H. Thomas, Lawrence Berkeley Laboratory, Occupational Health Office, 50A-5106, Engineering Division, Berkeley, CA 94720
70. V. D. Toneev, Laboratory of Theoretical Physics, Joint Institute for Nuclear Research, Head Post Office, PO Box 79, Moscow, USSR

71. W. Turchinets, Massachusetts Institute of Technology, R26-411,  
Cambridge, MA 02139
72. G. B. Yodh, Univ., of Maryland, College Park, MD 20742
73. Dr. B. Zeitnitz, Nuclear Research Center, Karlsruhe, W. Germany
- 74-103. Technical Information Center, PO Box 62, Oak Ridge, TN 37831